Characterization of Oil Slicks at Sea Using Remote Sensing Techniques

Eduardo Loos, Leslie Brown, Gary Borstad, Todd Mudge, Mar Álvarez
ASL Environmental Sciences, Inc.
1-6703 Rajpur Place, Victoria, BC, Canada V8M 1Z5
eloos@aslenv.com

***Abstract*—Oil slicks can be visually detected through remote sensing techniques because of sharp image contrast variations between the oil slicks and surrounding water. These contrast variations are usually due to the dampening of the water surface roughness caused not just by oil, but possibly also by freshwater runoff and biogenic surfactants (also called "biogenic look-alikes"), such as those due to phytoplankton blooms. Floating macroalgae can also alter the texture of the water surface and contribute to look-alikes. Using methodologies we developed and implemented in previous studies of oil spills using hyperspectral optical imagery, we have tested several algorithms for biogenic look-alikes and oil slick characterization from optical and RADAR sensors in order to improve operational monitoring of marine coastal areas for oil pollution. With the opportunity to use imagery acquired over the Deepwater Horizon oil spill in the Gulf of Mexico in 2010, we have demonstrated promising utility of optical imagery to assist in differentiating oil from RADAR look-alikes in low wind situations. We have demonstrated that the interpretation of false positives for oil slicks in RADAR imagery can be adequately assisted by the analysis of optical imagery. Furthermore, oil spill extent and slick thickness can be mapped and characterized using spaceborne imagery. This represents a major improvement over local observations of oil spill for emergency and mitigation actions by improving response time and providing a synoptic view of the impacted areas.**

***Index Terms*—Oil slick, satellite, remote sensing, RADARSAT, MERIS, Gulf of Mexico, Deepwater Horizon.**

I. Introduction

The use of remotely-sensed imagery for the characterization of oil slicks at sea is considered the best approach to accurately map the extent of oil spill events because of the temporal resolution and synoptic nature of the data [1]. Typically, active microwave sensors (RADAR) are favoured over visible/near-infrared optical sensors because of their ability to penetrate through clouds and rain. However, airborne or spaceborne visible/near-infrared sensors also provide information about oil slicks not available through RADAR analysis.

Oil slicks can be visually detected through remote sensing techniques because of sharp image contrast variations between the oil slicks and surrounding water. These contrast variations are usually due to the dampening of the water surface roughness caused not just by oil, but possibly also by freshwater runoff and biogenic surfactants, such as those due to phytoplankton blooms [2, 3].

A challenge for the accurate detection and mapping of oil from optical and RADAR sensors is the reduction of false positives or look-alikes. Because oil is detected from a dampening of Bragg scattering, natural phenomena which have this same effect can appear as look-alikes [4]. Among the most problematic of look-alikes are biogenic slicks caused by the release of surfactants by phytoplankton blooms at low wind speeds. Smaller biogenic look-alikes can also be expected by the dampening of surface waves by rafts of floating macroalgae, such as *Sargassum* in the Gulf of Mexico (GoM).

The presence of phytoplankton blooms and floating macroalgae is readily determined from optical imagery. In particular, MERIS has spectral bands that capture the fluorescence signal from chlorophyll a, and also the remnant red edge characteristic of surface or near surface algae [5]. MODIS also detects chlorophyll fluorescence but not the remnant red edge, and has lower spatial resolution (1km versus 300m for MERIS Full Resolution (FR)). Both sensors also detect chlorophyll based on the ratio of green to blue reflectance, but this algorithm is affected by blue absorption by dissolved organic matter.

In order to map the extent of and characterize oil spills, we have used coincident MERIS imagery to flag biogenic look-alikes in archived RADARSAT-1 and -2 imagery from the GoM. Wind speed and chlorophyll thresholds for the appearance of biogenic look-alikes were evaluated and algorithms were developed to detect and delineate the oil spills, as well as characterize their thicknesses.

II. Methods

Radiance and reflectance images were used in conjunction with wind data and GoM daily oil spill situation maps provided by NOAA (for the Deepwater Horizon Disaster in 2010) as input datasets showing overlays of oil polygons on optical imagery of the Gulf (Fig. 1). This information was helpful to separate look-alikes from oil. MERIS FR image data were obtained from the European Space Agency (ESA) as Level-1 at-sensor radiance in 15 spectral bands. Initially, radiance (Level-1) images were converted to reflectance (Level-2) images using either the FUB (Free University of Berlin) processor for Case-2 waters [6] or C2R (Case-2 Regional Processor) [7] in BEAM (ESA's image processing software). These processors were designed for coastal applications and allow for the presence of spectral absorption and scattering by

non-chlorophyllous suspended particulate matter and dissolved organic matter. However, the strong presence of sun glint on some of the MERIS FR images prevented us from using some of the reflectance images because the processors masked out the affected pixels. For look-alike analysis, simple viewing of the original RADARSAT datasets was adequate for comparisons with the optical imagery, however in the majority of cases we elected to also perform additional processing using IAPro software [8]. All images selected for the oil characterization analysis were reprojected in BEAM to Latitude/Longitude WGS-84.

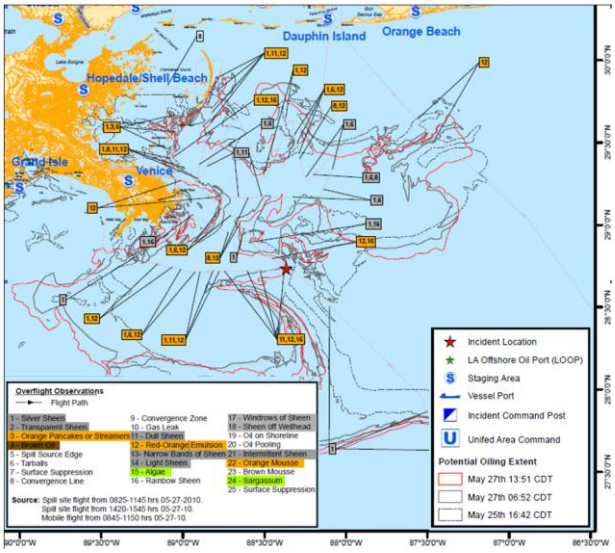

Fig. 1. Deepwater Horizon disaster situation map for May 27, 2010, showing the oil slick extent. Modified from ERMA [10].

Look-alikes analysis was performed by visual inspection of the coincident, co-located RADARSAT and MERIS images. The identification of biogenic look-alikes was in each case a subjective decision by the analyst, taking into account spatial patterns, temporal and spatial offsets, appearance in various optical image products (chlorophyll, FLH, MCI, RGB radiance, and RGB reflectance imagery), and for the GoM, the daily oil situation maps. Where look-alikes were identified, polygons were drawn manually to delineate each feature, using in some cases IAPro's SAR Ocean Feature Detection Tool (SOFDT) feature detection results to assist with the determination of feature boundaries. Wind speeds and chlorophyll concentrations associated with each feature were also evaluated in order to assess thresholds for look-alike occurrence for each of these parameters.

Further investigation led to mapping the extent of the oil spills and to the characterization of the oil thickness using MERIS optical imagery. We compared two different techniques. The first approach consisted of using spectral indices based on the ratio of spectral bands, in the blue (380-500 nm), red (600-760 nm), and near-infrared (760-2500 nm) parts of the electromagnetic spectrum (Table 1). The idea behind these algorithms was to highlight the fluorescence behaviour of surface oil slicks and the increased red reflectance by subsurface oil [9].

Table 1. Two different oil spill detection algorithms were tested. The Fluorescence Index (FI) used blue and red bands, whereas the Rotation-Absorption Index (RAI) used blue and infra-red bands.

Algorithm	Bands
Fluorescence Index (FI) $FI = \frac{R_B - R_R}{R_B + R_R}$ R_B = pixel radiance for the blue band R_R = pixel radiance for the red band	R_B = 490nm R_R = 665nm
Rotation-Absorption Index (RAI) $FI = \frac{R_B - R_{IR}}{R_B + R_{IR}} \frac{\|R\|}{\|R\|}$ where $\|R\| = \sqrt{\sum_{i=1}^{T} b_i^2}$ b = pixel radiance for image band T = total number of bands	R_B= 490nm R_{IR}= 885nm

The second approach consisted of using more complex ratios, again highlighting the fluorescence behaviour of oil slicks [11] (Table 2). Validation of the mapped areas was performed visually by overlaying oil spill vectors provided by the National Oceanic and Atmospheric Administration (NOAA). The characterization of the oil slick thickness consisted of classifying the outputs using the Spectral Angle Mapper (SAM) classifier. Classification accuracy assessment was performed using overflight observation maps of the oil spill provided by NOAA [12].

The characterization of the oil slick thickness used here (Table 3) was adapted from [11] and [12] in accordance with GoM overflight observations provided by NOAA's Environmental Response Management Application (ERMA) [10].

III. Results

Oil slicks on water present different optical behaviour depending on the sun's incidence angle and the satellite sensor's viewing geometry [13]. Oil slicks are not visible in sun glint-free images but can appear quite dark (negative contrast) under low to moderate sun glint or quite bright (positive contrast) under strong sun glint conditions [14].

For the GoM, no prior information was available for the occurrence of look-alikes, so the entire database of RADARSAT images (from MacDonald, Dettwiler and Associates Ltd.) was compared with MERIS imagery for the same time period. Of 198 RADARSAT scenes, 65 MERIS scenes were identified with overlapping footprints and acquisition times within 1 day of the RADARSAT data. 15 image pairs were identified in which common features were

visible in both types of imagery that were not apparently associated with oil (Fig. 2).

Table 2. MERIS radiance bands available for the oil slick characterization. Six band ratios were used according based on Svejkovsky & Muskat [11].

Band number	Band centre (nm)
1	412.5
2	442.5
3	490
4	510
5	560
6	620
7	665
8	681.25
9	708.75
10	753.75
11	760.625
12	778.75
13	865
14	885
15	900

Band Ratio
10/2
10/5
10/8
8/2
8/5
5/2

Table 3. Oil thickness classes adapted from Svejkovsky & Muskat [11] and NOAA [12].

Oil thickness T (mm)	Oil thickness class	Description
$T < 0.005$	Silver Sheen	A layer of oil that appears silvery or shimmers.
$0.005 \leq T < 0.050$	Rainbow Sheen	Sheen that reflects colours.
$0.050 \leq T < 1.000$	Red/brown Oil	Dark-coloured oil.
$T \geq 1.000$	Emulsions	Water-in-oil emulsion formed as oil weathers (mousse). Oil oriented in lines, windrows, or streaks (streamers). Weathered oil that has formed a pliable ball (tarballs).

The thresholded FI and RAI images obtained from the original radiance images were used only to assess the presence/absence of oil slicks (Fig. 3). The major advantage of using this algorithm is the fact that thresholds can be generated for one single band-ratioed image that highlights the fluorescence behaviour of surface and subsurface oil slicks by incorporating the radiometric characteristics of two distinct channels (blue and red for FI and blue and infra-red for RAI). At this point, a simple validation was performed visually by overlaying ERMA oil slick boundaries on the thresholded imagery.

Oil thickness was obtained from supervised classification algorithms modified from Sveijkovsky & Muskat [11]. Generally, the classification algorithm was not able to correctly isolate sun glint-affected areas from immediately-adjacent areas. Hence, sun glint areas had to be incorporated into the training procedure separately and labeled accordingly (Fig. 4). The most reliable source of ground-truth data was ERMA [10]. *In situ* oil characteristics were based on a simple visual assessment collected from daily flights over the affected areas. Accuracy assessment of the classified images was performed using randomly-generated samples (individual pixels) due to the limited number of ground-truth observations. Randomly-generated samples were then assigned a reference class based on their locations, overflight observations, and spectral signatures obtained from the images. SAM outputs presented considerably accurate classifications of oil slick thickness on water, as indicated in Table 4.

Table 4. Overall accuracy of the SAM classifications for four MERIS images analysed using 100 random samples (pixels).

Image date	Overall accuracy (%)	Kappa Coefficient
May 24 2010	38	0.13
May 27 2010	82	0.62
July 14 2010	64	0.50
July 20 2010	69	0.45

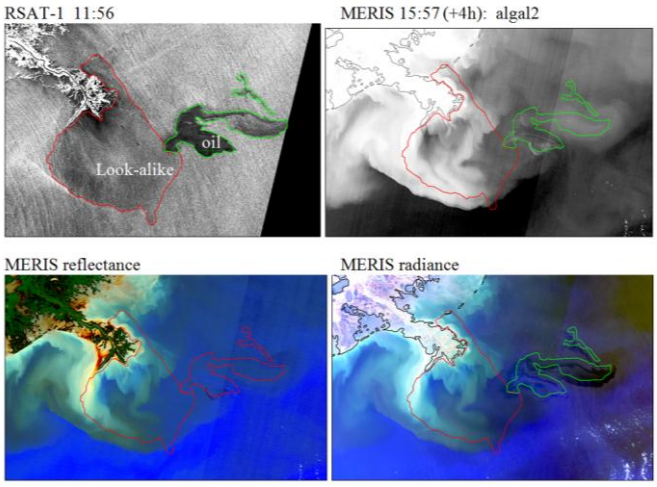

Fig. 2. Look-alikes datasets containing both oil and oil look-alikes in RADARSAT-1 (RSAT-1) and MERIS images. Note that the MERIS algal2 is a product providing chlorophyll concentration. Look-alike vectors were hand-drawn and oil vectors were obtained from ERMA[10].

IV. Conclusion

Overall, the methods tested here yielded significant maps of location, extent, and thickness of oil spills. We noticed that the interpretation of false positives for oil slicks in RADAR imagery can be assisted by the examination of optical imagery. Specifically, multispectral spaceborne optical sensors of medium spatial resolution, such as MERIS FR (300 m), provide sufficient spatial, spectral, radiometric, and temporal detail to aid in the characterization of oil slicks as long as there are no clouds over the area of interest in the image. Thus, the accuracy of oil thickness classification using optical imagery ranged from 38% to 82%.

Acknowledgment

This work is part of a larger project for the Canadian Space Agency (CSA) through the Earth Observation Application Development Program (EOADP) that also includes

MacDonald, Dettwiler and Associates Ltd. (MDA), and the Centre for Cold Ocean Resources Engineering (C-CORE).

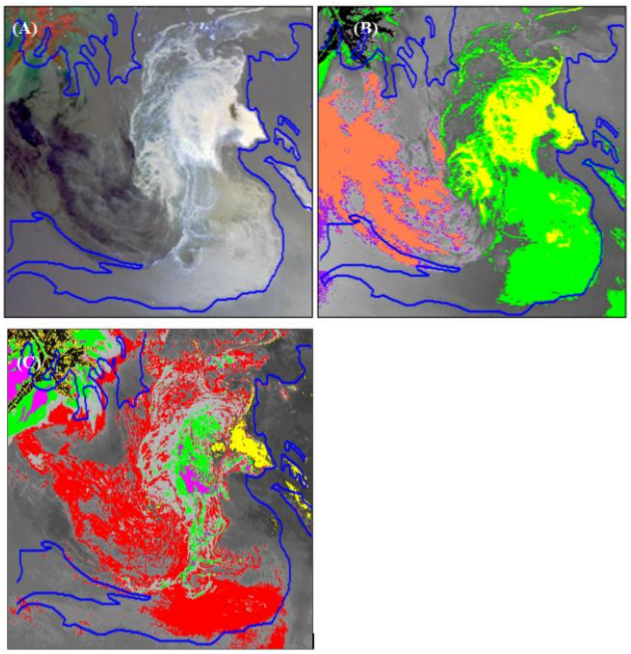

Fig. 3. Oil delineation results. (A) Original true-colour MERIS radiance composite, (B) thresholded FI image showing potential surface oil spill areas, (C) thresholded RAI image showing potential subsurface oil. Oil vectors obtained from ERMA [14].

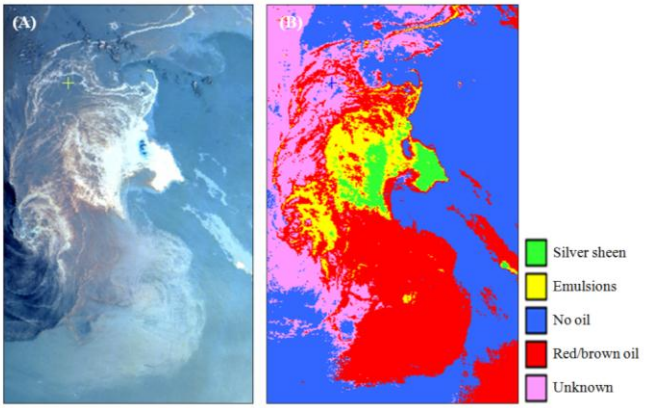

Fig. 4. (A) False-colour MERIS band-ratio image (red = band 10/band 2, green = band 10/band 5, blue = band 10/ band 8), (B) SAM classification output with five oil slick thickness classes based on overflight observations and surface spectral signatures.

REFERENCES

[1] Kvenvolden, K. A. and Cooper, C.K. 2003. Natural seepage of crude oil into the marine environment. Geo-Marine Letters, 23(3-4): 140–146.

[2] Lin, I.-I.; Wen, L.; Liu, K.; Tsai, W; Liu, A.K. 2002. Evidence and quantification of the correlation between RADAR backscatter and ocean colour supported by simultaneously acquired in situ sea truth. Geophysical Research Letters, 29(10): 1464, doi:10.1029/2001GL014039.

[3] DiGiacomo, P.M.; Washburn, L; Holt, B.; Jones, B.H. 2004. Coastal pollution hazards in southern California observed by SAR imagery: Stormwater plumes, wastewater plumes, and natural hydrocarbon seeps. Marine Pollution Bulletin, 49: 1013–1024.

[4] Brekke, C. and Solberg, A.H.S. 2005. Oil spill detection by satellite remote sensing, Remote Sensing of Environment, 95(1): 1-13.

[5] Gower, J.; Hu, C.; Borstad, G.; King, S. 2006. Ocean-color satellites show extensive lines of floating *Sargassum* in the Gulf of Mexico. IEEE Transactions on Geoscience and Remote Sensing, 44(12): 3619-3625.

[6] Schroeder, T.; Schaale, M.; Fischer, J. 2007. Retrieval of atmospheric and oceanic properties from MERIS measurements: A new Case-2 water processor for BEAM. International Journal of Remote Sensing, 28(24): 5627-5632.

[7] Doerffer, R and Schiller, H. 2007. The MERIS Case 2 water algorithm. International Journal of Remote Sensing, 28 (3-4): 517-535.

[8] Wolfe, J. and Robson, M. 2009. Image Analyst Pro (IAPro) for SOIN User Manual. DRDC Ottawa Technical Memorandum, 2009-083.

[9] Lennon, M.; Mariette, V.; Coast, A.; Vergeque, V.; Mouge, P.; Borstad, G.A.; Willis, P.; Kerr, R.; Alvarez, M. 2003. Detection and mapping of the November, 2002 PRESTIGE tanker oil spill in Galicia, Spain, with the airborne multispectral CASI sensor. In: 3rd EARSEL Workshop on Imaging Spectroscopy, Herrsching, 13-16 May 2003.

[10] ERMA. 2012. Environmental Response Management Application Gulf Response. Retrieved from: http://gomex.erma.noaa.gov/.

[11] Svejkovsky, J. and Muskat, J. 2006. Real-time detection of oil slick thickness patterns with a portable multispectral sensor. Final Report submitted to the U.S. Department of the Interior, Minerals Management Service, Herndon, VA, July 31, 2006. 37 p.

[12] NOAA. 1996. Aerial observations of oil at sea – HAZMAT Report 96-7. Retrieved from http://response.restoration.noaa.gov/oil-and-chemical-spills/oil-spills/resources/open-water-oil-identification-job-aid.html.

[13] Hu, C.; Li, X.; Pichel, W.G.; Muller-Karger, F.E. 2009. Detection of natural oil slicks in the NW Gulf of Mexico using MODIS imagery. Geophysical Research Letters, 36, L01604, doi:10.1029/2008GL036119.

[14] Hu, C.; Li, X.; Pichel, W.G. Detection of Oil Slicks using MODIS and SAR Imagery. 2011. In: Morales, J.; Stuart, V.; Platt, T.; Sathyendranath, S. (Eds.). Handbook of Satellite Remote Sensing Image Interpretation: Applications for Marine Living Resources Conservation and Management. EU PRESPO and IOCCG, Dartmouth, Canada, p. 21-34.